Bioorganic & Medicinal Chemistry Letters 22 (2012) 4660–4664

Contents lists available at SciVerse ScienceDirect

Bioorganic & Medicinal Chemistry Letters

journal homepage: www.elsevier.com/locate/bmcl

Novel 2-(2-(benzylthio)-1*H*-benzo[*d*]imidazol-1-yl)acetic acids: Discovery and hit-to-lead evolution of a selective CRTh2 receptor antagonist chemotype

Julien Pothier, Markus A. Riederer, Oliver Peter, Xavier Leroy, Anja Valdenaire, Carmela Gnerre, Heinz Fretz *

Actelion Pharmaceuticals Ltd, Gewerbestrasse, 16, CH-4123 Allschwil, Switzerland

ARTICLE INFO

Article history:
Received 11 May 2012
Accepted 23 May 2012
Available online 1 June 2012

Keywords:
CRTh2
DP2
Prostaglandin
Asthma
Rhinitis

ABSTRACT

Hit-to-lead evolution of 2-(2-((2-(4-chlorophenoxy)ethyl)thio)-1*H*-benzo[*d*]imidazol-1-yl)acetic acid (1), discovered in a high-throughput screening campaign as a novel chemotype of CRTh2 receptor antagonist, is presented. SAR development as well as in vitro and in vivo DMPK properties of selected representatives of substituted 2-(2-(benzylthio)-1*H*-benzo[*d*]imidazol-1-yl)acetic acids are discussed.

Prostaglandin D2 (PGD_2), a major metabolite of arachidonic acid, is predominantly involved in the physiological response to allergy. It is released at high concentration by immunoglobulin E activated mast cells upon allergen challenge[1] and was demonstrated to activate two G-protein coupled receptors (GPCRs), the classical DP1 receptor and the recently discovered chemoattractant receptor-homologous molecule expressed on T-helper 2 cells (CRTh2 also known as DP2) receptor.[2] CRTh2 activation leads to the recruitment of granulocytes and Th2 cells by chemotaxis[3] to the inflammation site and has been in almost all cases demonstrated to be pro-inflammatory.[4,5] Furthermore it is now well established that antagonizing selectively the CRTh2 receptor could be useful in the treatment of asthma and other inflammatory diseases such as allergic rhinitis.[6–10] Herein, we describe the discovery and development of a novel CRTh2 antagonist chemotype series.

Our search for a selective CRTh2 receptor antagonist was initiated by screening our GPCR biased in-house compound collection by means of an in vitro fluorescent imaging plate reader (FLIPR™, Molecular Devices) assay. The assay was performed in a 384-well plate format. Human embryonic kidney cells (HEK-293) stably expressing the human (*h*)CRTh2 receptor under the control of the CMV promoter from a single insertion of the expression vector pcDNA5 (Invitrogen), were challenged with PGD_2 (10 nM concentration) in the presence and absence of test compounds. In these transformed cells, PGD_2 induces release of calcium (Ca^{2+}) from intracellular Ca^{2+} stores. Changes of such intracellular Ca^{2+} concentrations were measured by monitoring changes in fluorescence emission at λ_{ex} = 488 nm and λ_{em} = 540 nm of the added cytoplasmic Ca^{2+} indicator Fluo-3 and Pluronic F-127 (Molecular Probes) upon Ca^{2+} complexation. This screening effort revealed hit compound **1** (Fig. 1) consisting of a 2-(2-((substituted)alkylthio)-1*H*-benzo[*d*]imidazol-1-yl)acetic acid core. **1** antagonizes PGD_2 induced *h*CRTh2 activation with an IC_{50} = 6.6 μM. Furthermore, we could demonstrate PGD_2 competitive binding of **1** to the *h*CRTh2 receptor with an IC_{50} = 1.5 μM. The receptor binding assay was performed again with HEK-293 cells expressing *h*CRTh2 receptor employing the agonist radioligand [^{3}H]PGD_2 (2.5 nM, 169 Ci/mmol).

The carboxylic acid is a common functionality to all endogenous prostanoids as well as many of the published prostanoid receptor agonists and antagonists.[11] Alike, the carboxylic acid of **1** was shown to be essential for *h*CRTh2 receptor interaction and therefore was kept throughout the optimization process. The focus of the first set of benzimidazole analogues was directed towards the initial thiobenzimidazole hit core (X = S, R = H) addressing part **A** of **2**. As indicated (Fig. 1), part **A** represents a (C_1–C_4)alkyl chain connected through a linker group Y to various Z residues.

General synthetic pathways are outlined in Scheme 1(A) for unsubstituted (R = H) and in 1(B) for unsymmetrically R-substituted benzimidazole scaffold (R≠H), respectively. Typically, starting 2-chlorobenzimidazole (**3**) was reacted with *tert*-butylbromoacetate and potassium carbonate in refluxing acetone to form *tert*-butyl 2-(2-chloro-benzimidazol-1-yl) acetate (**4**). Substitution of the chlorine atom by means of thiourea in refluxing methanol yielded

* Corresponding author. Tel.: +41 61 565 6208; fax: +41 61 565 8901.
E-mail address: heinz.fretz@actelion.com (H. Fretz).

0960-894X/$ - see front matter © 2012 Elsevier Ltd. All rights reserved.
http://dx.doi.org/10.1016/j.bmcl.2012.05.087

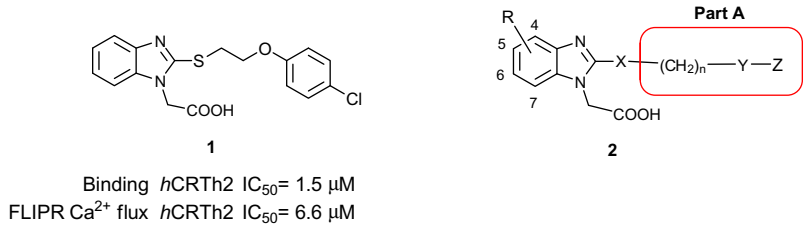

Figure 1. Structure of initial high-throughput screening hit **1** and general formula **2**, indicating the positions investigated during the hit-to-lead phase.

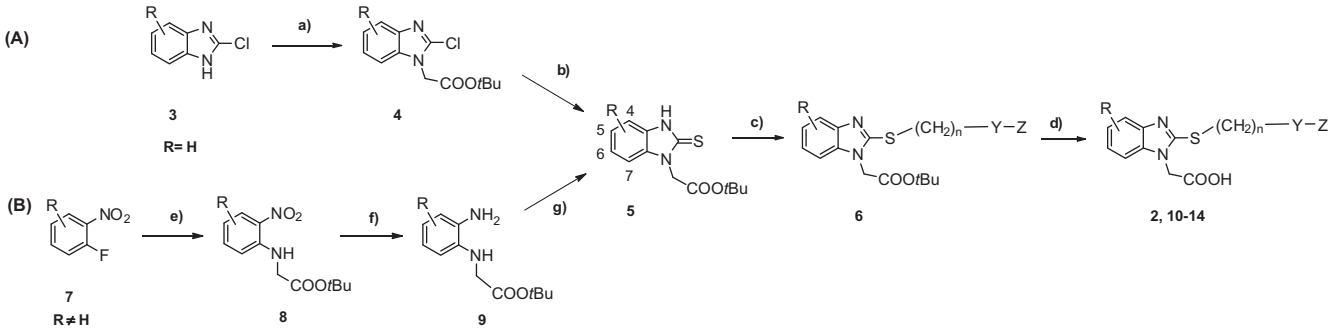

Scheme 1. Reagent and conditions: (a) *tert*-butylbromoacetate, K_2CO_3, acetone, reflux (50–93%); (b) thiourea, methanol, reflux (45–98%); (c) Br-$(CH_2)_n$-Y–Z, K_2CO^3, acetone, reflux; or HO-$(CH_2)_n$-Y–Z, (=NC(O)O*t*Bu)$_2$, Ph^3P, THF; (d) TFA, DCM, rt; (e) $NH_2CH_2CO_2tBu$ hydrochloride, Na_2CO_3, DMSO, 50 °C (44–96%); (f) H_2, 5% mol Pd/C, THF, rt; (g) 1,1′-thiocarbonyldiimidazole, THF, rt (41–73% over 2 steps).

tert-butyl 2-(2-thioxo-2,3-dihydro-1*H*-benzo[*d*]imidazol-1-yl) acetate **5**,[12] which was then *S*-alkylated either with Br-$(CH_2)_n$-Y–Z in the presence of potassium carbonate in refluxing acetone, or in a Mitsunobu reaction with HO-$(CH_2)_n$-Y–Z in presence of di-*tert*-butylazodicarboxylate and triphenylphosphine in THF to give **6**. Subsequent hydrolysis of *tert*-butyl acetate **6** with TFA in dichloromethane yielded the expected thiobenzimidazole-1-acetic acid **2** and **10–12**.

Depicted in Scheme 1(B) is a regioselective approach, devised to provide benzimidazole analogue **2** with a substituent R other than hydrogen at any of the positions C(4), C(5) or C(6) of the core, avoiding cumbersome chromatographic separations of regioisomers. Accordingly R substituted 1-fluoro-2-nitrobenzene (**7**) and *tert*-butyl glycinate hydrochloride reacted in the presence of sodium carbonate in DMSO at 50 °C to give the substituted 2-((2-nitrophenyl)amino)acetate **8**.[13] Palladium-catalyzed hydrogenolysis of the nitro group with H_2 in THF under atmospheric pressure yielded amine **9**, which then was converted without purification by means of 1,1′-thiocarbonyl-diimidazole to the corresponding R substituted *tert*-butyl 2-(2-thioxo-2,3-dihydro-1*H*-benzo[*d*]imidazol-1-yl)acetate **5**. Subsequent *S*-alkylation and final deprotection gave the desired products **13** and **14**.

Following our screening cascade, the competitive radioligand displacement assay described above was used as a test system to establish the structure activity relationship (SAR) for all synthesized potential *h*CRTh2 antagonists. The FLIPR assay was used as a secondary assay in order to give evidence that the compounds are truly antagonizing the effect of agonist PGD_2 on the *h*CRTh2 receptor. The results from both assays are reported as IC_{50} values. Selectivity of the antagonists towards the DP1 receptor was determined using a competitive receptor binding assay with CHO (Chinese Hamster Ovary) cells expressing high levels of recombinant DP1 receptor, employing [^{3}H]PGD_2 as ligand.[14] Plasma as well as chemical stabilities were assessed by incubating the antagonists in rat plasma for up to 4 h, in simulated gastric fluid (SGF) for 1 h and simulated intestinal fluid (SIF) for 4 h.[15] Recovery of unchanged parent was determined by LC-MS. Potent (binding IC_{50}<100 nM), selective and stable antagonists were further verified in a competitive radioligand displacement assay in the presence of 0.5% human serum albumin (HSA) in order to identify those antagonists that retained potency under conditions where binding to blood proteins occurs. The positives were subsequently tested in an eosinophil shape change (ESC) assay.[16,17] In brief, human eosinophils were isolated from whole blood of healthy volunteers and were subsequently stimulated with 15 nM PGD_2 in the presence of 50% human plasma (HP) at 37 °C, for 5 min. Stimulation was stopped by adding fixation solution and increase in light scattering reflecting changes in cell shape was measured by flow cytometry. A dose dependent inhibition of this shape change could be demonstrated with potent antagonists by pre-incubating the cells with the increasing concentrations of antagonist for 10 min prior to stimulation with PGD_2.

A preliminary SAR was established with compounds **2a**–**2r** (Table 1). The original hit **1** (Z = 4-chlorophenyl) was found to be three times less potent than **2a** with Z = phenyl. Also, **2b** and **2c** containing the larger bicyclic substituents Z = naphth-2-yl and naphth-1-yl respectively, were considerably less potent. No clear correlation could be ascribed to the length of the *n*-alkyl chain and the observed potency. The potency of the compounds was dependant on both, the type of connecting group Y and the length of the *n*-alkyl chain, for example Y = CH_2, Z = phenyl and *n* = 0, was found to be most potent (**2h,** IC_{50} = 388 nM) in this first series. An additional CH_2 (*n* = 1) led to more than a twofold drop of potency (**2g**), whereas an almost complete regain was observed by further elongating *n*-alkyl to *n* = 2, as shown with **2f**. Optimal *n*-alkyl chain length was observed if ethyl (*n* = 2) was combined with Y = O (**2a**), or *n*-propyl (*n* = 3) with Y = NH (**2i**). An unexpected but interesting discovery was made within the homologous alkanoate series. An almost linear increase in potency was observed from ethyl propanoate up to ethyl hexanoate (**2n**–**2q**), **2q** being the most potent

Table 1
*h*CRTh2 receptor binding IC_{50} values of compounds **2a–2r**

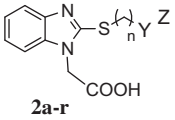

2a-r

Compound	*n*	Y	Z	*h*CRTh2 binding buffer IC_{50}[a] (nM)
2a	2	O	Phenyl	590
2b	2	O	2-Naphthyl	2500
2c	2	O	1-Naphthyl	2000
2d	3	O	Phenyl	786
2e	4	O	Phenyl	1400
2f	2	CH_2	Phenyl	475
2g	1	CH_2	Phenyl	881
2h	0	CH_2	Phenyl	388
2i	3	NH	Phenyl	2690
2j	2	NH	Phenyl	7690
2k	4	CH_2	Methyl	1360
2l	3	CH_2	Methyl	1240
2m	2	CH_2	Methyl	2370
2n	1	CH_2	COOEt	11,400
2o	2	CH_2	COOEt	4410
2p	3	CH_2	COOEt	2360
2q	4	CH_2	COOEt	1010
2r	3	CH_2	CONHEt	>10,000

[a]Values are the mean of two or more experiments.

(IC_{50} = 1010 nM). Absolutely no interaction with the receptor was observed for the corresponding ethylamide **2r**.

Subsequently, the sulfur atom of the thiobenzimidazole core (**2**, X = S) was systematically replaced by X = O, CH_2, and NH. All compounds obtained were considerably less potent than the corresponding thiobenzimidazole analogues (data not shown). Oxidation of the sulfur atom to the corresponding 2-sulfinyl- or 2-sulfonyl-1*H*-benzo[*d*]imidazole (X = SO, or SO_2) analogues gave at least a fivefold drop in potency (data not shown).

With this information, we decided to focus on further exploring **2h**. Subsequently, tolerability and effect of a substituent R at the phenyl ring were investigated (**10**, Table 2). A positional scanning was carried out comprising in parts the Topliss scheme for aromatic substitutents,[18] first substituting the hydrogen atom at position C(2), C(3) and C(4) with chloro, methoxy, methyl, bromo, and methoxycarbonyl (Table 2). The latter was included at this stage because of the discovery made with alkanoate homologues **2n–2q**. However, an inconclusive SAR was obtained. The corresponding 4-chloro, 4-methoxy and 4-methyl analogue **10a**, **10d** and **10g**, respectively, showed similar potencies and were found to be approximately two times more potent than **2h**. Bromine at any of the three positions led to a minor loss of potency keeping the same ranking order compared with respective chloro substitution. Clearly less tolerated was the 4-methoxycarbonyl (**10m**). Furthermore, substituents at position 2 generally tended to result in less potent compounds (**10c**, **10f**, **10i, 10l**) within a series. Compared to **2h**, a greater than five times lower IC_{50} value was obtained with 3-methoxy substitution (**10e**).

The effect of a second substituent R at the phenyl ring was studied in a combinatorial approach. Only readily available building blocks containing two substituents were selected and introduced according to Scheme 1. Thereby building blocks were chosen where a substituent like chloro, methoxy, methyl, bromo, or methoxycarbonyl as in **10a–10o**, respectively, was present in any combination with a second substitutent such as chloro, methoxy, methyl, or bromo, to give for example **11a** to **11j** (Table 2). In this study, the 3,4-dichloro analogue **11a** was found two times less potent than the respective mono-substituted 4- or 3-chloro analogue **10a** and **10b**.

Table 2
*h*CRTh2 receptor binding IC_{50} values of compounds **10a–12d**

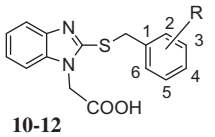

10-12

Compound	Substituent *R* at				*h*CRTh2 binding buffer IC_{50}[a] (nM)
	C(2)	C(3)	C(4)	C(5)	
10a	H	H	Cl	H	160
10b	H	Cl	H	H	186
10c	Cl	H	H	H	370
10d	H	H	OMe	H	210
10e	H	OMe	H	H	72
10f	OMe	H	H	H	1100
10g	H	H	Me	H	220
10h	H	Me	H	H	105
10i	Me	H	H	H	810
10j	H	H	Br	H	220
10k	H	Br	H	H	370
10l	Br	H	H	H	580
10m	H	H	CO_2Me	H	10,600
10n	H	CO_2Me	H	H	450
10o	CO_2Me	H	H	H	520
11a	H	Cl	Cl	H	380
11b	Cl	H	H	Cl	470
11c	OMe	H	H	Me	1200
11d	OMe	H	H	Cl	740
11e	OMe	H	H	OMe	1600
11f	OMe	H	H	CO_2Me	29
11g	Br	CO_2Me	H	H	2900
11h	H	CO_2Me	Br	H	980
11i	H	Br	H	CO_2Me	330
11j	Br	H	H	CO_2Me	45
12a	OMe	H	H	CO_2iPr	150
12b	OMe	H	H	C(O)Me	8
12c	H	H	H	C(O)Me	230
12d	OMe	H	H	CH(OH)Me	2200[b]

[a]Values are the mean of two or more experiments.
[b]Racemic.

Table 3
*h*CRTh2 receptor binding and FLIPR IC_{50} values of compounds **13a–13h**

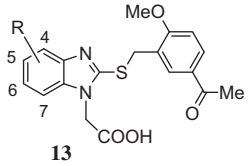

13

Compound	Substituents Rat			*h*CRTh2 binding buffer IC_{50}[a] (nM)	$(Ca^{2+})_i$ flux FLIPR *h*CRTh2 IC_{50}[a] (nM)
	C(4)	C(5)	C(6)		
13a	F	H	H	5	10
13b	H	F	H	2	5
13c	H	H	F	45	89
13d	H	NO_2	H	2	3
13e	H	CF_3	H	3	5
13f	H	$MeSO_2$	H	41	50
13g	H	Me(O)C	H	33	63
13h	H	H(O)C	H	4	9

[a]Values are the mean of two or more experiments.

Comparable values were measured for 2,5-dichloro analogue **11b** and 2-chloro substituted **10c**. Superimposing a phenyl ring substituted with A at C(2) and a phenyl ring substituted with B at C(3) implies a 2,3- or a 2,5-disubstitution pattern if both substituents A and B are combined on one phenyl ring. In our subsequent

Table 4
*h*CRTh2 receptor binding and FLIPR IC_{50} values of compounds **14a–14k**

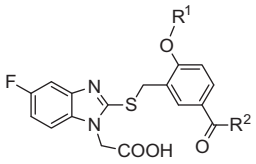

14

Compound	R^1	R^2	*h*CRTh2 binding buffer IC_{50}[a] (nM)	$(Ca^{2+})_i$ flux FLIPR *h*CRTh2 IC_{50}[a] (nM)
14a	Et	Me	4	5
14b	*n*Pr	Me	5	9
14c	*n*Bu	Me	9	12
14d	Me	Ph	1.7	4
14e	Me	NHEt	16	15
14f	Me	NHBu	16	15
14g	Me	NHBn	59	94
14h	Me	NEt_2	72	130
14i	Me	NBnEt	495	725
14j	Me	Morpholino	107	91
14k	Me	Indolin-1-yl	3	4

[a] Values are the mean of two or more experiments.

Table 5
Comparative in vitro profiles of representative key antagonists

Assay	CRTh2 receptor antagonist			
	12b	**13b**	**14f**	**14k**
*h*CRTh2 Bdg in buffer IC_{50} (nM)	9	2	16	3
*h*CRTh2 FLIPR IC_{50} (nM)	25	5	15	4
*h*CRTh2 Bdg in HSA[a] IC_{50} (nM)	2	14	81	8
ESC in 50% plasma IC_{50} (nM)	16	5	41	51
*h*DP1Binding IC_{50} (nM)	>10000	>10000	>10000	>10000
*h*TP FLIPR IC_{50} (nM)	>25000	>25000	nd[b]	nd
MW (Da)	370	388	445	491
$LogD_{7.4}$	−1.1	−0.8	0.1	0.3
Solubility (ng/ml)				
0.1 M HCl	575	484	670	158
Phosphate buffer pH 7	602	399	719	812
Tris buffer pH9	583	583	>750	789
Chemical stability				
SGF% parent after 1 h	92	95	94	100
SIF% parent after 4 h	100	100	78	100
Human plasma stability				
% parent (4 h)	100	100	100	93
in vitro ADME profile				
CL_{int} (RLM) (μl/min/mg protein)	17	60	60	91
CL_{int} (HLM) (μl/min/mg protein)	0	13	7	2
CL_{int} (RHepa) (μl/min/10^6 cells)	10	20	6	12
CYP2D6 IC_{50} (μM)	>50	>50	>50	>50
CYP3A4 (Mid)[c] IC_{50} (μM)	37	10	4	5
CYP3A4 (Test)[c] IC_{50} (μM)	>50	15	7	13
CYP2C9 IC_{50} (μM)	24	>50	6	2

[a] 0.5% Human serum albumin.
[b] No data.
[c] Substrates used: Mid = midazolam, Test = testosterone.

studies we mainly focused on the 2,5-substitution pattern. For example, unifying 2-methoxy of **10f** (IC_{50} 1100 nM) with 3-chloro of **10b**, or 3-methoxy of **10e**, or 3-methyl of **10h**, in one molecule lead to a substantial loss of binding affinity as demonstrated for **11c**, **11d**, and **11e**, respectively. However, to our surprise 2-methoxy, as in **10f**, combined with 3-methoxycarbonyl of **10n** in a 2,5-disubstitution pattern yielded **11f** the most potent compound (IC_{50} = 29 nM) so far. The positional scanning, whereupon hydrogen was substituted with bromine at C(2), C(4) and C(5) as in **11g–11j**, afforded **11j** with IC_{50} = 45 nM. That finding actually confirmed (a) the positive *ortho* effect induced with this 2,5-disubstitution pattern and (b) that this pattern is superior over all other investigated combinations.

Replacing the initial 5-methoxycarbonyl with other groups, for example more suitable alkoxycarbonyl groups such as 5-isopropoxycarbonyl, (CO_2*i*Pr, **12a**) caused a fivefold decrease in potency. Further attempts to replace 5-methoxycarbonyl led to the discovery of **12b** with an IC_{50} = 8 nM, containing 5-methylcarbonyl instead. The importance of a carbonyl group at C(5) in combination with a 2-methoxy substituent could be impressively demonstrated, as **12b** was found ~30 times more potent than **12c** and >200 times more potent than 1-hydroxyethyl analogue **12d**.

Attaching a substituent R to the benzimidazole core **13** generated highly potent compounds (Table 3), binding to the *h*CRTh2 receptor with IC_{50} values in the single digit nM range, especially if R represents a strong electron-withdrawing group at C(5) such as fluorine, nitro, trifluoromethyl or formyl.

Finally, a small library was produced exploiting in more detail scope and limitations of the positions R^1 and R^2 of **14** (Table 4). It was found that for R^1 besides Me **(11f**, **12b**, **13b**) also the C_2-C_{44}-alkyl homologues (**14a**, **14b** and **14c)** were tolerated. These compounds were shown to inhibit PGD_2 binding to the *h*CRTh2 receptor comparable to **13b** with IC_{50} values <10 nM. Further modifications of R^2 resulted in **14d** displaying an IC_{50} = 1.7 nM. So far, this was the most potent compound generated in this whole series. However, more emphasis was put on replacing the metabolically critical ketone or ester functionality. As illustrated with **14g–14j**, increasing bulkiness of the alkylamino part leads to decreasing potency of the antagonists. Interestingly, regain of the full inhibitory potential was observed by attaching the constrained bicyclic indolin-1-yl residue as in **14k**. *h*CRTh2 antagonism of selected compounds was assessed in the aforementioned (Ca^{2+}) flux FLIPR assay (Tables 3 and 4). All compounds were confirmed as antagonists. Binding and FLIPR data correlate with comparable potencies for the high affinity compounds, whereas a two- to fourfold shift is observed for the weaker antagonists. In order to address protein binding, the binding assay was performed in the presence of 0.5% HSA prior to further profiling. Antagonists displaying no or only a minor shift in potency in presence of HSA were tested for inhibitory activity in the functional ESC assay, whereas antagonists displaying a major shift under those conditions were not further profiled.

The properties of four selected representatives of this novel chemotype lead series are summarized in Table 5. Comparable profiles were obtained concerning the activity on the *h*CRTh2 receptor for **12b**, **13b** and **14k** under various assay conditions, **14f** performed slightly weaker. High selectivity towards the *h*DP1 and *h*TP receptor could be achieved. Low to medium molecular weight (MW) ranging from 370 to 491 Da, and measured $LogD_{7.4}$ values ranging from −1.1 to +0.3 gave rise to highly soluble compounds in aqueous buffer solutions. Chemical as well as plasma stability

Table 6
Comparative in vivo pharmacokinetic[a] profile of selected CRTH2 antagonists

Compound	AUC (ngxh/ml)	CL (ml/min/kg)	V_{ss} (L/kg)	$T_{1/2}$ (h)	*F* (%)
12b	2360	20	1.1	2.5	27
13b	919	36	1.2	0.9	19

[a] Male Wistar rats (3 animals for each experiment), *iv* dose 1 mg/kg, *po* dose 10 mg/kg as a solution.

appeared not to be an issue, the selected compounds were found stable under the various conditions, for example >90% of parent was recovered after incubation in SGF for 1 h. Upon exposure to SIF for 4 h, **14f** turned out to be slightly less stable (78% recovery of parent).

Compound **12b** displayed low intrinsic clearance (Cl_{int}) in rat liver microsomes (RLM) and suspended hepatocytes (RHepa) with values of 17 μl/min/mg protein and 10 μl/min/10^6 cells, respectively. No turnover was measured in human liver micorosomes (HLM). All three other analogues systematically showed higher turnover in RLM and HLM. In RHepa, Cl_{int} values for **13b**, **14f** and **14k** were within a factor of two compared to **12b**.

All four selected representatives were weak inhibitors of the cytochrome P450 isoform CYP2D6 with IC_{50} values higher than 50 μM. Moderate inhibition of CYP2C9 was measured for **14f** with an IC_{50} of 6 μM, whereas **12b**, **13b** and **14k** were weaker inhibitors with IC_{50} values of 24 μM, >50 μM and 28 μM, respectively. A similarly moderate inhibition pattern was observed on CYP3A4 with **12b** displaying the weakest effect.

Pharmacokinetic studies with prototypical compounds **12b** and **13b** (Table 6) were carried out in Wistar rats at intravenous and oral doses of 1 and 10 mg/kg, respectively. After oral administration of **12b**, a significant exposure (AUC) was reached (2360 ng.h/mL), whereas the AUC for **13b** was more than two times lower. Both derivatives showed decent oral bioavailability with 27% and 19%, respectively. The des-fluoro derivative **12b** displayed a moderate systemic plasma clearance of 20 ml/min/kg, while the value for the fluorinated **13b** was twice as high. The same trend in Cl_{int} was observed when comparing data obtained with **12b** and **13b** in RLM and RHepa.

As described for many acidic drugs (e.g., warfarin, aspirin) a small apparent volume of distribution at steady state V_{ss} of about 1 L/kg was determined for both candidates.

In essence, the systematic optimization combined with serendipitous findings during the evolution of the screening hit led to the discovery of a structurally novel lead series comprising potent and selective *h*CRTh2 receptor antagonists. Representative examples were shown to display encouraging in vitro and in vivo DMPK properties. Therefore, this lead series was considered useful and proposed for further lead optimization and development.

Acknowledgments

The authors thank A. Jonuzi, P. Risch, B. Butscha, J. Giller, B. Lack, S. Brand for valuable technical support, B. Capeleto, R. Bravo, S. Delahaye, H. Kletzl for providing DMPK data, K. Hilpert for fruitful discussions and J. Williams for the proofreading of the manuscript.

Supplementary data

Supplementary data associated with this article can be found, in the online version, at http://dx.doi.org/10.1016/j.bmcl.2012.05.087.

References and notes

1. Murray, J. J.; Tonnel, A. B.; Brash, A. R. N. *Engl. J. Med.* **1986**, *315*, 800.
2. Gervais, F. G.; Cruz, R. P.; Chateauneuf, A.; Gale, S.; Sawyer, N.; Nantel, F.; Metters, K. M.; O'Neill, G. P. *J. Allergy Clin. Immunol.* **2001**, *108*(6), 982.
3. Hirai, H.; Tanaka, K.; Yoshie, O.; Ogawa, K.; Kenmotsu, K.; Takamori, Y.; Ichimasa, M.; Sugamura, K.; Nakamura, M.; Takano, S.; Nagata, K. *J. Exp. Med.* **2001**, *193*, 255.
4. Pettipher, R. *Br. J. Pharmacol.* **2008**, *153*, S191.
5. Kostenis, E.; Ulven, T. *Trends Mol. Med.* **2006**, *12*, 148.
6. Pettipher, R.; Hansel, T. T.; Armer, R. *Nat. Rev. Drug Disc.* **2007**, *6*, 313.
7. Chen, J. J.; Budelsky, A. L. *Prog. Med. Chem.* **2011**, *50*, 49.
8. Burgess, L. E. *Ann. Rep. Med. Chem.* **2011**, *46*, 119.
9. Schuligoi, R.; Sturm, E.; Luschnig, P.; Konya, V.; Philipose, S.; Sedj, M.; Waldhoer, M.; Peskar, B. A.; Heinemann, A. *Pharmacology* **2010**, *85*, 372.
10. Pettipher, R.; Hansel, T. T. *Prog. Respir. Res. Basel Karger* **2010**, *39*, 193.
11. Hirata, T.; Narumiya, S. *Chem. Rev.* **2011**, *111*(10), 6209.
12. Arima, Hideki.; Tomioka, Kenichi; Yamada, Toshimitsu; Murase, Kiyoshi *J. Med. Chem.* **1986**, *29*, 386.
13. McFarlane Michael, D.; Moody David, J.; Smith David, M. *J. Chem. Soc., Perkin Trans. 1* **1988**, *3*, 691.
14. Boie, Y.; Sawyer, N.; Slipetz, D. M.; Metters, K. M.; Abramovitz, M. *J. Biol. Chem.* **1995**, *270*, 18190.
15. Asafu-Adjaye, E. B.; Faustino, P. J.; Tawakkul, M. A.; Anderson, L. W.; Yu, L. X.; Kwon, H.; Volpe, D. A. *J. Pharm. Biomed. Anal.* **2007**, *43*(5), 1854.
16. Stubbs, V. E.; Schratl, P.; Hartnell, A.; Williams, T. J.; Peskar, B. A.; Heinemann, A.; Sabroe, I. *J. Biol. Chem.* **2002**, *277*(29), 26012.
17. Sabroe, I.; Hartnell, A.; Jopling, L. A.; Bel, S.; Ponath, P. D.; Pease, J. E.; Collins, P. D.; Williams, T. J. *J. Immunol.* **1999**, *162*(5), 2946.
18. Topliss, J. G. *J. Med. Chem.* **1972**, *15*, 1006.